

Functional Role of Neuroendocrine-Specific Protein-Like 1 in Membrane Translocation of GLUT4

Takaaki Ikemoto,¹ Takamitsu Hosoya,² Kumi Takata,¹ Hiroshi Aoyama,³ Toshiyuki Hiramatsu,² Hirotaka Onoe,¹ Masaaki Suzuki,⁴ and Makoto Endo⁵

OBJECTIVE—In skeletal muscles, dantrolene inhibits the exercise-induced membrane translocation of GLUT4. It has been postulated that the inhibitory action of dantrolene on Ca²⁺ release from the sarcoplasmic reticulum (SR) causes inhibition of exercise-induced glucose uptake; however, the precise mechanism has not been adequately studied.

RESEARCH DESIGN AND METHODS—We discovered that dantrolene can bind to skeletal-type neuroendocrine-specific protein-like 1 (sk-NSP11) with photoreactive dantrolene derivatives. In sk-NSP11-deficient muscles, we examined the change in glucose uptake and the membrane translocation of GLUT4. In addition, we examined the change in blood glucose and also measured the glycogen level in both isolated and in situ skeletal muscles after electrical stimulation using our mutant mouse.

RESULTS—In sk-NSP11-deficient muscles, exercise-induced glucose uptake was totally abolished with no change in insulin-induced glucose uptake. The Ca²⁺ release mechanism and its inhibition by dantrolene were completely preserved in these muscles. The expression of GLUT4 in the mutant muscles also appeared unchanged. Confocal imaging and results using the membrane isolation method showed that exercise/contraction did not enhance GLUT4 translocation in these sk-NSP11-deficient muscles under conditions of adequate muscle glycogen consumption. The blood glucose level in normal mice was reduced by electrical stimulation of the hind limbs, but that in mutant mice was unchanged.

CONCLUSIONS—sk-NSP11 is a novel dantrolene receptor that plays an important role in membrane translocation of GLUT4 induced by contraction/exercise. The 23-kDa sk-NSP11 may also be involved in the regulation of glucose levels in the whole body. *Diabetes* 58:2802–2812, 2009

From the ¹Functional Probe Research Laboratory, RIKEN Center for Molecular Imaging Science, Kobe, Japan; the ²Department of Biological Information, Graduate School of Bioscience and Biotechnology, Tokyo Institute of Technology and SORST (Solution Oriented Research for Science and Technology), Japan Science and Technology Agency, Yokohama, Japan; the ³Institute of Molecular and Cellular Biosciences, University of Tokyo, Tokyo, Japan; the ⁴Molecular Imaging Medicinal Chemistry Laboratory, RIKEN Center for Molecular Imaging Science, Kobe, Japan; and the ⁵Faculty of Health and Medical Care, Saitama Medical University, Saitama, Japan. Corresponding author: Functional Probe Research Laboratory, tikemotoriko@riken.jp.

Received 19 May 2009 and accepted 17 August 2009. Published ahead of print at <http://diabetes.diabetesjournals.org> on 31 August 2009. DOI: 10.2337/db09-0756.

© 2009 by the American Diabetes Association. Readers may use this article as long as the work is properly cited, the use is educational and not for profit, and the work is not altered. See <http://creativecommons.org/licenses/by-nc-nd/3.0/> for details.

The costs of publication of this article were defrayed in part by the payment of page charges. This article must therefore be hereby marked "advertisement" in accordance with 18 U.S.C. Section 1734 solely to indicate this fact.

Contraction/exercise is an activating factor for glucose transport in skeletal muscle. Skeletal muscle stores glucose in large capacity as glycogen. Insulin is another direct activator of glucose transport in skeletal muscle, and thus insulin and exercise are the most physiologically important regulators of glucose metabolism in skeletal muscle (1,2). Despite the physiological importance of exercise for glucose transport in skeletal muscle, the molecular mechanisms that underlie this function remain unclear.

Dantrolene sodium is a well-known inhibitor of excitation-contraction coupling by inhibiting Ca²⁺ release from the sarcoplasmic reticulum (SR) (3,4), and it has been used as a very effective drug for the treatment of porcine and human malignant hyperthermia (5–7). It has been reported that dantrolene also has an inhibitory effect on exercise-induced glucose uptake in skeletal muscle, without effects on insulin-induced glucose uptake (8–12). Exercise-induced glucose uptake is considered to be the result of translocation of GLUT4 from internal stores to the cell membrane, and in this mechanism, Ca²⁺ release from Ca²⁺ stores (SR) is thought to be critically involved (11,13,14). Therefore, it may be natural to assume that the inhibitory effect of dantrolene on glucose transport results from the inhibitory action of dantrolene on Ca²⁺ release. However, no previous study has adequately focused on the inhibitory mechanism of dantrolene on glucose metabolism.

Considering the unique action of dantrolene on Ca²⁺ release in skeletal muscle, efforts have been made to identify a molecular target of dantrolene in the SR using appropriate dantrolene derivatives (15–17). In the current report, we demonstrate that a newly discovered 23-kDa protein photolabeled with dantrolene derivatives is a skeletal muscle type of neuroendocrine-specific protein-like 1 (sk-NSP11) in mice (18). We had expected that this protein might be a regulatory factor of physiological Ca²⁺ release from the SR of skeletal muscle. However, there was no functional change in the Ca²⁺ release mechanism in skeletal muscle lacking muscle transcripts of the sk-NSP11 gene. Instead, exercise-induced glucose uptake in skeletal muscle was totally abolished in the mutant mice, although insulin-induced glucose uptake was preserved. This report indicates that the 23-kDa sk-NSP11 is a novel dantrolene receptor that plays a role in translocation of GLUT4 in skeletal muscle.

RESEARCH DESIGN AND METHODS

Photoaffinity analysis using membrane fractions from skeletal muscles.

In the first photoaffinity analysis, we used terminal cisternae fractions from ICR mice (12 weeks, male) by sucrose density gradient centrifugation according to the reported protocol (19). For mutant mice (Fig. 1C), membrane

of 3.2% CHAPS, 2.0 mol/l NaCl, and 20 mmol/l PIPES/Tris (pH 7.0). After 30 min of stirring, the sample was centrifuged and filtered. The affinity-purified antibody against sk-NSP1 protein was incubated with the solubilized sample for 16 h. Then, 20 μ l of agarose-bound protein A was added to the sample and incubated for 2–4 h at 4°C. Protein A agarose-absorbed complexes were washed five times with repetitive centrifugation. Protein bound with [¹²⁵I]GIF-0082 was also visualized with BAS-2500 as mentioned above.

Mice lacking NSP1. Because exon 5 of the NSP1 gene is the muscle transcript-specific exon (18), exon 5-targeted disrupted mice (two lines) were obtained from Lexicon Pharmaceuticals. Homozygous mutant mice were generated by intercrossing of heterozygotes. PCR genotyping was used to distinguish the wild-type and targeted alleles. The primers OYC10-1 and OYC10-7 listed here amplified the product from the wild-type allele, and primers NEO3B and OYC10-1 amplified the product from the targeted allele: NEO3B 5'-GCAGCGCATCGCCTTCTATC-3', OYC10-1 5'-CCCAGCTCCAA-CAGGCCTC-3', and OYC10-7 5'-CCACTCTCTGGCCAGC-3'. All experiments in this report used 8- to 12-week-old male mice after fasting for 15–17 h.

Measurement of contractile response in intact muscles and Ca²⁺ release in skinned muscles. The change in tension of intact muscles was measured in accordance with previous reports (16,24,25). The measurement of Ca²⁺ release using fura-2 from the SR in skinned skeletal muscles (extensor digitorum longus [EDL]) is also described in detail elsewhere (26,27).

Analysis of 2-deoxy-2-[¹⁸F]fluoro-D-glucose uptake in skeletal muscles. 2-Deoxy-2-[¹⁸F]fluoro-D-glucose ([¹⁸F]FDG) was provided by the chemical synthesis laboratory of the Innovated Biochemical Research Institute (Kobe, Japan). It is possible to measure the change in glucose uptake into the cell with a very low concentration of [¹⁸F]FDG because of its high radioactivity; however, we observed that glucose inhibited [¹⁸F]FDG uptake (this data can be found in supplemental Fig. 3, available in the online appendix at <http://diabetes.diabetesjournals.org/cgi/content/full/db09-0756/DC1>). Because glucose is suspected to be an important factor for GLUT4 translocation, we applied electrical stimulation to the muscle in the presence of glucose (5.6 mmol/l) and then incubated the muscle in glucose-free solution containing [¹⁸F]FDG (Fig. 3A). Briefly, after tension recording for 15 min with (20 V, 0.5 ms duration, 125 Hz, for 320 ms, 3 s⁻¹; or 25 Hz for 2 s, 3 s⁻¹) or without electrical stimulation in normal physiological salt solution, the experimental solution was exchanged for glucose-free physiological salt solution containing [¹⁸F]FDG (0.375 MBq/ml). After 2, 5, or 10 min incubation, [¹⁸F]FDG was washed out with glucose-free physiological salt solution. Then the muscles were freeze-dried and the muscle weights measured. The remaining radioactivity derived from [¹⁸F]FDG was measured by a 2480 Wizard (2) automatic γ -counter (PerkinElmer). In some of these experiments, after measurement of radioactivity, the muscle glycogen was measured as described below.

Confocal microscopy. EDL muscles excised from wild-type or mutant mice were incubated in physiological salt solution with or without electrical stimulation for 15 min (25 Hz for 2 s, 5 s⁻¹). Insulin (2 units) was injected 10 min before isolation of muscles and then excised. The thin muscles were fixed by 3.5% freshly depolymerized paraformaldehyde for 2 h. After washing with Tris-buffered saline (TBS; pH 7.4), single muscles were treated with 0.05% Triton X-100 for 15 min and then with 5% skim milk for 15 min. Then the muscles were incubated in TBS containing several primary antibodies (anti-GLUT4 and -dystrophin [Chemicon] and anti-ryanodine receptor [Affinity BioReagents]) overnight. After four washes to remove the primary antibodies, muscles were incubated for 3 h with Alexa Fluor 488 or 568 goat anti-rabbit or mouse IgG (H+L; Invitrogen) diluted with TBS at 1:400. Confocal images for double-labeled muscle were collected on a Digital Eclipse C1 system equipped with a TE2000-E microscope (Nikon). To compare the localization of GLUT4, dystrophin, ryanodine receptor, NSP1, and actin, separate images (two channels) recorded at high magnification ($\times 100$; numerical aperture 1.49 lens, oil) were imported into EZ-C1 software (Nikon) and visualized. Quantification of the confocal data are further described in Figs. 4A and 5E.

Analysis of GLUT4 translocation in isolated membranes. The hind limb muscles were quickly isolated from fasting and anesthetized wild-type or mutant mice. Membrane fractionation of muscles was carried out in accordance with previous reports (28,29) with modification. We analyzed GLUT4 translocation in fractions 1–3 and LiBr-treated membrane fractions from skeletal muscles with specific antibodies (there are additional data available in the supplemental material).

Measurement of blood glucose in whole mouse. The blood glucose level of anesthetized mice was measured with a Glucocard-Diameter- α (GT-1661; Arkray). First, in control, insulin, and electrical stimulation mouse groups, blood glucose levels were measured after fasting for 16–17 h (at time = 0) by cutting the tail. After 10 min, glucose containing saline was injected (1.67 mg/g), and then blood glucose levels were measured at 30, 50, and 80 min in all groups. Electrical stimulation (50 V, 25 Hz for 2 s, 5 min⁻¹) was delivered from a platinum wire directly inserted into the hind limbs at 30–50 min and at 60–80 min. Insulin (2 units) was injected intraperitoneally at 20 min. In some

of these experiments, at 0, 80, and 95 min (15 min after the last measurement of blood glucose levels), the rectus femoris muscle was quickly isolated and cut into small pieces to measure muscle glycogen. The sample was freeze-dried and the weight measured. The unsolubilized fraction from the sample, in 80% ethanol per 1 mol/l KOH solution, was treated with thermostable α -amylase and amyloglucosidase. The glucose enzymatically produced in the sample was measured with a glucose assay kit (Invitrogen).

Data analysis. Data are the means \pm SEM. Paired data sets were tested using Student paired *t* test. Multiple comparisons were analyzed using one-way ANOVA for repeated measurements followed by Fisher PLSD (protected least significant difference) post hoc test. *P* < 0.05 was considered statistically significant.

RESULTS

Photoaffinity labeling of dantrolene-binding proteins in skeletal muscle. As shown in our previous report (20), dantrolene derivatives GIF-0430 and [¹²⁵I]GIF-0082 can specifically label proteins of low molecular weight in rabbit terminal cisternae fractions by photoirradiation. In mouse skeletal muscle, larger molecules were also photo-labeled with [¹²⁵I]GIF-0082, but labeling of the 23-kDa protein was not as clearly observed compared with other dantrolene derivative labeling of larger-molecular weight proteins (Fig. 1A, lanes 2–7; supplemental Fig. 1A–F). Unlike dantrolene and other dantrolene derivatives, GIF-0166 and GIF-0192 enhanced Ca²⁺ release (supplemental Fig. 1J and K), as observed by the replacement of [¹²⁵I]GIF-0082 binding (Fig. 1A, lanes 5 and 6). On the other hand, [¹²⁵I]GIF-0136, another type of dantrolene derivative, showed little effect on Ca²⁺ release (supplemental Fig. 1I and K), but it did not recognize the 23-kDa protein; labeling of larger molecules was similar to other derivatives (supplemental Fig. 1H). Sequence analysis of this 23-kDa protein from rabbit resulted in an amino acid sequence including GSKVADLLYWKDART (the first 15 NH₂-terminal amino acid residues), which is almost the same as RTN2-C (30) in humans or NSP1 (18) in mice.

Polyclonal antibodies against mouse NSP1 made the [¹²⁵I]GIF-0082-labeled 23-kDa protein precipitate (Fig. 1B), and the radioactivity was reduced in the preparation labeled in the presence of nonradioactive GIF-0082 (10 μ l serum) (Fig. 1B), indicating that the GIF-0082-photolabeled 23-kDa protein in the skeletal muscle of the mouse is sk-NSP1.

Ca²⁺ release from the SR in sk-NSP1-deficient skeletal muscles. To clarify the physiological role of sk-NSP1 as a dantrolene receptor, we used mutant mice lacking sk-NSP1. The deletion of sk-NSP1 in the mutant skeletal muscle was confirmed by the lack of fluorescent signals from GIF-0373 coupled with GIF-0430 in the membrane fraction from the mutant muscle (Fig. 1C) and also by the lack of specific antibody detection (Fig. 1D and E). We initially assumed that the function of sk-NSP1 might be crucial for the regulatory mechanism of the ryanodine receptor–Ca²⁺ release channel in excitation-contraction coupling (22,31). Unexpectedly, in NSP1-deficient muscle, we observed no abnormalities in twitch tension, time to peak, half relaxation time, and 125 Hz-induced submaximum tension (Fig. 2) or in the frequency-tension relationship (supplemental Fig. 2A and B). In skinned muscles of mutant mice, the Ca²⁺-induced Ca²⁺ release mechanism also operated normally (supplemental Fig. 2C). Furthermore, the inhibitory effects of dantrolene and GIF-0082 on Ca²⁺ release were clearly preserved (Fig. 2A and B and supplemental Fig. 2C). Therefore, the sk-NSP1 protein appears to play no role in regulation of Ca²⁺ release in skeletal muscle.

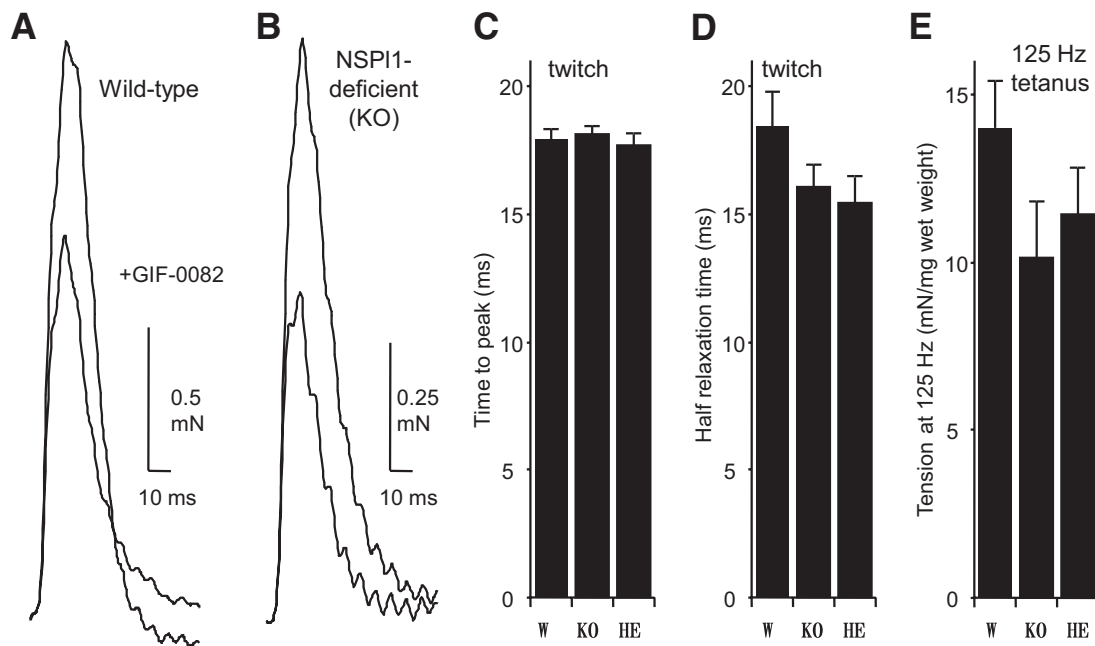


FIG. 2. Contractile response of dantrolene receptor-deficient skeletal muscles. *A* and *B*: Typical recordings of twitch contractions in the diaphragm muscles from wild-type (*A*) and sk-NSP11-deficient mutant (*B*) mice in the presence or absence of Gif-0082 (20 μ M). *C* and *D*: Time to peak tension (*C*) and half relaxation time (*D*) were measured during the twitch tension of the diaphragm muscles evoked by 0.2 Hz of electrical stimulation (20 V, 0.5 ms duration) for wild-type (W; $n = 25$) and mutant (sk-NSP11-deficient [KO], $n = 19$; and sk-NSP11 heterozygous [HE], $n = 14$) mice. *E*: Submaximum tension of the diaphragm muscle evoked by electrical stimulation at 125 Hz (wild type, $n = 17$; sk-NSP11 deficient, $n = 8$; heterozygous, $n = 4$).

Glucose transport in sk-NSP11-deficient muscles. We analyzed glucose uptake in NSP11-deficient skeletal muscle because dantrolene is a potent inhibitor of exercise-induced glucose uptake (10–12). First, we measured uptake of [18 F]FDG, a glucose analog, into skeletal muscle cells. Uptake of [18 F]FDG immediately followed 15 min of electrical stimulation, which adequately reduced muscle glycogen (Fig. 3C). In wild-type skeletal muscle, uptake of [18 F]FDG during a 5-min incubation increased more than twofold after electrical stimulation of 125 or 25 Hz (Fig. 3D and E), and this enhancement of uptake activity was inhibited by Gif-0082 (data not shown) as well as by Gif-0166, which potentiates Ca^{2+} release (Fig. 3E) (22). On the other hand, uptake of [18 F]FDG was not increased at all by stimulation in both homozygotes (sk-NSP11 deficient) and heterozygotes (Fig. 3E). Thus, exercise-induced glucose uptake in skeletal muscle cells was seriously impaired in sk-NSP11-deficient skeletal muscle.

Translocation of GLUT4 in sk-NSP11-deficient muscles. In skeletal muscle from our mutant mice, no significant change in the total amount of GLUT4 was observed (Fig. 1D). Because exercise-induced glucose uptake is considered to be the result of membrane translocation of GLUT4, we examined translocation of GLUT4 in muscles from these mutants. We compared the presence of GLUT4 in the surface membrane with that deep within the muscle cells using confocal microscopy (Fig. 4). Because dystrophin in skeletal muscle cells is concentrated near the sarcolemma to mechanically stabilize the membrane (32,33), the induction of GLUT4 in the dystrophin-abundant section should indicate enhancement of GLUT4 translocation into the sarcolemma. Indeed, GLUT4 was markedly increased at the dystrophin-abundant section when wild-type skeletal muscle was treated with insulin (Fig. 4B vs. D) or electrically stimulated (Fig. 4B vs. F). On the other hand, in NSP11-deficient skeletal muscle, al-

though insulin also increased GLUT4 near the sarcolemma (Fig. 4C vs. E), distribution of GLUT4 was almost unchanged by electrical stimulation (Fig. 4C vs. G). Analysis of multiple sections (Fig. 4A) confirmed that electrical stimulation did not enhance GLUT4 translocation in NSP11-deficient muscles (Fig. 4G and H). These results are consistent with the view that the reduction in [18 F]FDG uptake in skeletal muscle lacking sk-NSP11 (Fig. 3E) resulted from the impairment of GLUT4 translocation. Although it seemed that the action of insulin in sk-NSP11-deficient muscles was much greater than that in wild-type muscles (Fig. 4H and I), no statistically significant difference was found between them ($P = 0.545$ at 0 μ M; $P = 0.220$ at 0.5 μ M).

It has been reported that GLUT4 in the internal membrane is translocated not only into the sarcolemma, but also into the transverse-tubule membrane in skeletal muscles (34–36). We compared the locations of GLUT4 with those of the ryanodine receptor, which is closely associated with and functionally linked to the dihydropyridine receptors on the transverse-tubule membrane (37), in wild-type and mutant muscles. After electrical stimulation in wild-type muscles, a large quantity of the GLUT4 was located near the transverse tubules, whereas the remaining GLUT4 showed no translocation from the unstimulated state (Fig. 5A and B). As shown in Fig. 5F, the maximum fluorescence from GLUT4 shifted in response to stimulation from the center between two transverse tubules (A-I junctions) to mostly one side of the transverse tubules. In NSP11-deficient mice, two fluorescence peaks were clearly separated without stimulation (Fig. 5G), and on stimulation, the peak of GLUT4 was shifted to the center of the A-I junctions as in the wild-type mice without stimulation (Fig. 5G), demonstrating abnormalities in distribution and translocation of GLUT4 in relation to the transverse-tubule membrane in the mutant mice.

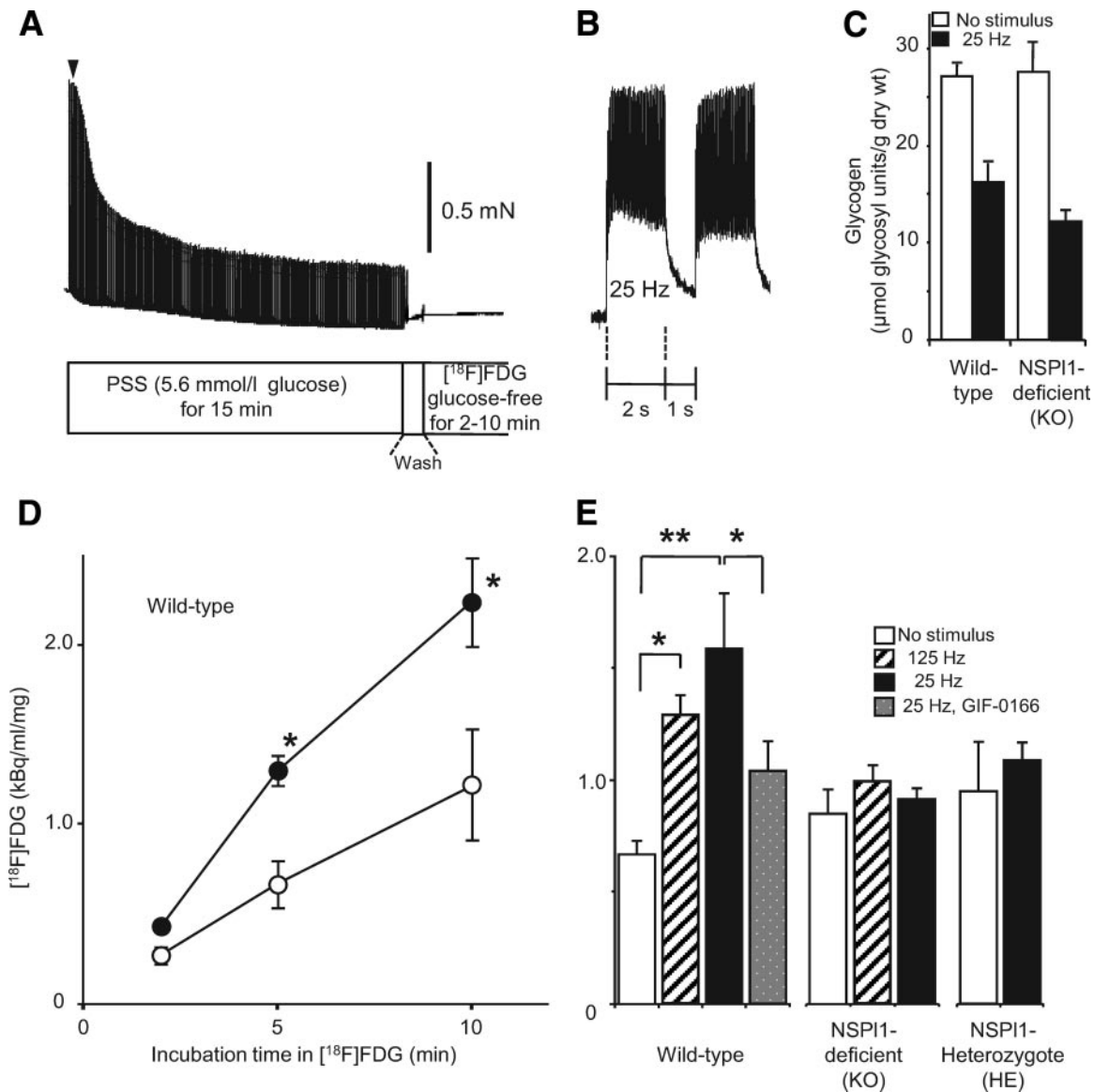


FIG. 3. Uptake of [¹⁸F]FDG in skeletal muscles. **A:** Experimental protocol for [¹⁸F]FDG uptake in skeletal muscles (EDL). After recording contractions evoked by electrical stimulation in normal glucose solution, we washed skeletal muscles with glucose-free solution (Wash), and then incubated them in solution containing [¹⁸F]FDG for 2, 5, or 10 min. PSS, physiological salt solution. **B:** Typical recording of fused tetanus induced by stimulation (25 Hz, 0.5 ms duration for 2 s, 3 s⁻¹) at the time point indicated by the filled arrowhead in **A**. **C:** Glycogen content after electrical stimulation. After the procedure shown in **A** with a 5-min incubation with glucose-free solution, muscle glycogen content was compared with electrical stimulation (25 Hz for 15 min, *n* = 19 for wild type; *n* = 12 for sk-NSP11 deficient) or without electrical stimulation (*n* = 12 for wild type; *n* = 11 for sk-NSP11 deficient). The results contain data from samples after measurement of [¹⁸F]FDG uptake. **D:** Time-dependent increase of [¹⁸F]FDG uptake in skeletal muscles (EDL). Radioactivity in EDL muscles from wild-type mice after incubation with [¹⁸F]FDG for 2, 5, or 10 min was compared with (●) or without (○) electrical stimulation (*n* = 4–5). **E:** [¹⁸F]FDG uptake during 5-min incubation after electrical stimulation (15 min at 125 Hz or 25 Hz) in wild-type and mutant (sk-NSP11-deficient and -heterozygous) EDL muscles (*n* = 4–14 for wild-type, *n* = 4–18 for sk-NSP11 deficient, *n* = 4–18 for sk-NSP11 heterozygous). **P* < 0.05, ***P* < 0.02.

GLUT4 translocation in isolated membrane. To further study abnormalities of GLUT4 translocation, we compared the content of GLUT4 among different fractions of isolated transverse-tubule membranes between wild-type and sk-NSP11-deficient mice. In our isolation method, membrane fractions 1 and 2 contained α-2 dihydropyridine receptor located in the transverse-tubule membrane and Na-K ATPase in both transverse tubules and sarcolemma (Fig. 6A and B) (29). Thus, membrane fractions 1 and 2 were thought to be the cell membrane-rich fractions. LiBr-treated membrane is characterized as a fraction that contains a high concentration of intracellular membrane (28,29).

Insulin (2 units) and electrical stimulation increased the GLUT4 content in membrane fractions 1 and 2, whereas

they decreased it in LiBr-treated membrane (Fig. 6C and E, G and I, K and M) for the wild-type mice, with no change in the sk-NSP11 content in either fraction (Fig. 6O–Q). On the other hand, no significant difference was observed in the sk-NSP11-deficient mice when their muscles were electrically stimulated (Fig. 6D and F vs. L and N), although the action of insulin was preserved (Fig. 6D and F vs. H and J). These data directly indicate that in muscles lacking sk-NSP11, contraction/exercise does not induce translocation of GLUT4, which causes the impairment of exercise-induced glucose uptake.

Relationship between exercise-induced glucose uptake and blood glucose level in whole mice. We examined the change in blood glucose levels in our mutant

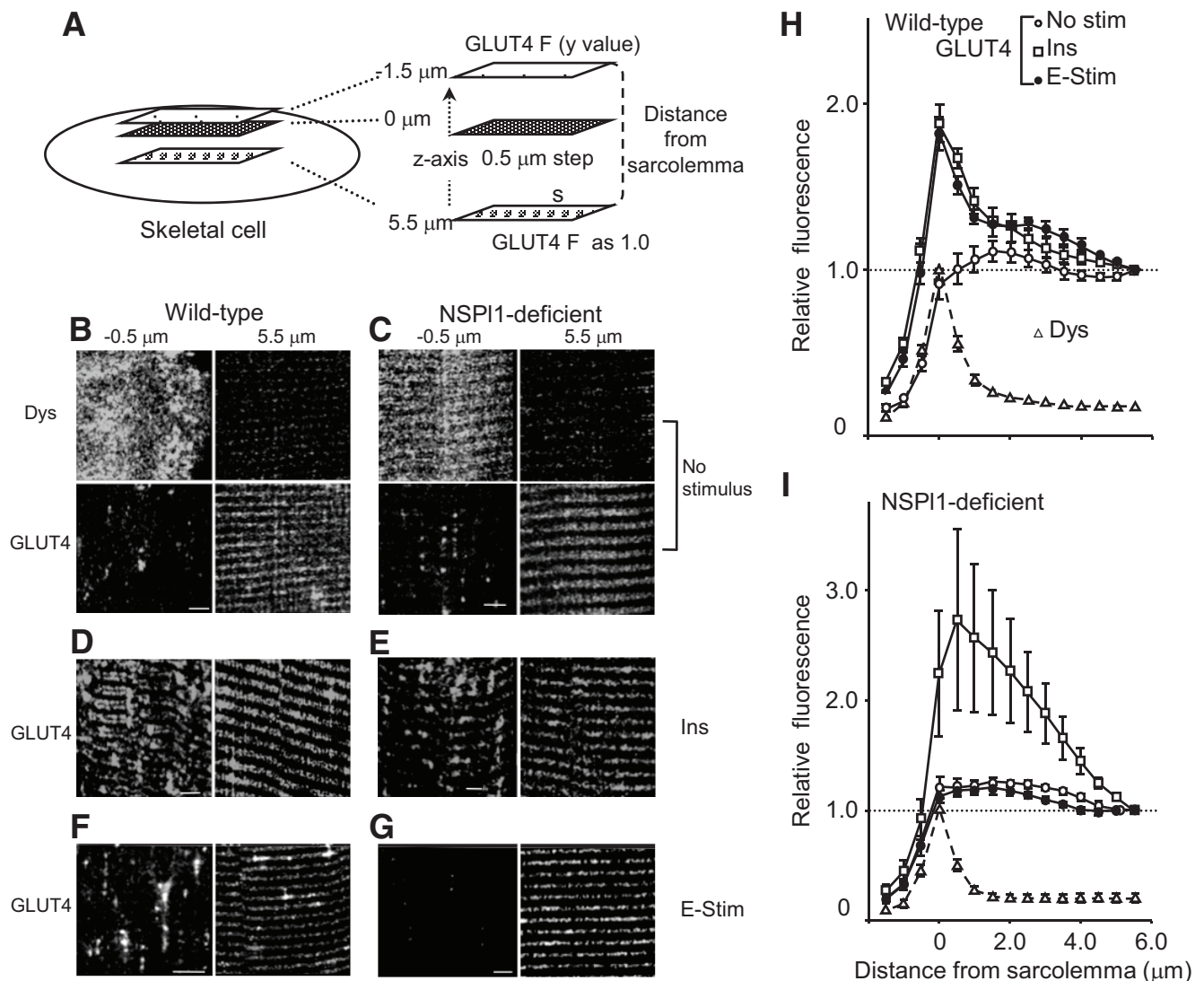


FIG. 4. Confocal imaging of GLUT4 immunofluorescence in mouse skeletal muscles. **A:** Quantification of GLUT4 translocation in the sarcolemma. We obtained images of the area surrounding a portion of a single muscle from one outer surface to the other ($60\text{--}100\ \mu\text{m} \times 60\ \mu\text{m}$, 512×512 pixels/dimension) every $0.5\ \mu\text{m}$ along the z -axis. Then, the intensity of fluorescence with Alexa Fluor 488-conjugated secondary antibody against anti-dystrophin (dys) was analyzed from a recorded image at every acquired section (S; $30\ \mu\text{m} \times 30\ \mu\text{m}$), and the depth at its maximum value was defined as one side of the cell surface ($0\ \mu\text{m}$). The intensity of fluorescence with Alexa Fluor 568-conjugated secondary antibody against anti-GLUT4 from the -1.5 (outer surface) to $5.0\ \mu\text{m}$ was normalized to that at $5.5\ \mu\text{m}$ and was plotted in **H** and **I**. **B–G:** Typical images from wild-type (**B**, **D**, and **F**) or sk-NSP11-deficient (**C**, **E**, and **G**) muscles; a series of confocal images of dystrophin-derived (**B** and **C**) and GLUT4-derived immunofluorescence in EDL muscle were recorded from the outer surface of the muscle cell ($-1.5\ \mu\text{m}$) to the deep cell ($5.5\ \mu\text{m}$). Distributions of GLUT4 in control muscles (No stimulus) (**B** and **C**), after insulin treatment (Ins; 2 units) (**D** and **E**), and after electrical stimulation for 15 min (E-stim; 20 V, 25 Hz) (**F** and **G**). Bar = $5\ \mu\text{m}$. **H** and **I:** Analysis of multiple sections of GLUT4 translocation in the wild-type (**H**) and sk-NSP11-deficient muscles (**I**), as shown in **A**. Control muscle (no stimulus); insulin treated (Ins; 2 units); electrical stimulation (E-stim; 25 Hz). \circ , no stimulus; \square , insulin treated; \bullet , electrical stimulation. The change in intensity of the dystrophin immunofluorescence was normalized to its peak value at $0\ \mu\text{m}$ (Δ). $n = 8\text{--}9$, in each experiment. Dys, dystrophin.

mice to see whether the deficiency of exercise-induced glucose uptake in skeletal muscle was accompanied by changes in the regulation of glucose level in the whole body. In both wild-type and mutant mice, injection of a high-glucose solution increased the blood glucose level rapidly, and insulin (2 units) dramatically reduced it (Fig. 7). In wild-type mice, electrical stimulation of hind limbs also reduced the blood glucose level, although its extent was much lower than with insulin injection (Fig. 7A). In sk-NSP11-deficient mice and even in the sk-NSP11-heterozygous mice, long-lasting electrical stimulation of hind limbs caused no change in blood glucose levels (Fig. 7B and C), although even in situ, muscle glycogen was reduced in both mutant types of muscles (Fig. 7D). At 15 min after termination of electrical

stimulation (at 95 min), the glycogen content in all muscle types was recovered at the same extent as without fasting (Fig. 7D). Thus, glycogen metabolism was not significantly changed in sk-NSP11-deficient muscles. Taken together, the whole mutant mouse, which has a defect in exercise-induced glucose uptake in skeletal muscles, also has less ability to reduce blood glucose levels on contraction/exercise.

Abnormality in muscles from sk-NSP11-heterozygous mice. As shown in Figs. 3 and 7, exercise-induced glucose uptake was abolished in muscle from sk-NSP11-heterozygous mice, where the total amount of sk-NSP11 was markedly reduced ($<50\%$) (Fig. 1D). We investigated whether the reduction in sk-NSP11 caused an abnormality of its characteristic distribution in muscle from sk-NSP11-

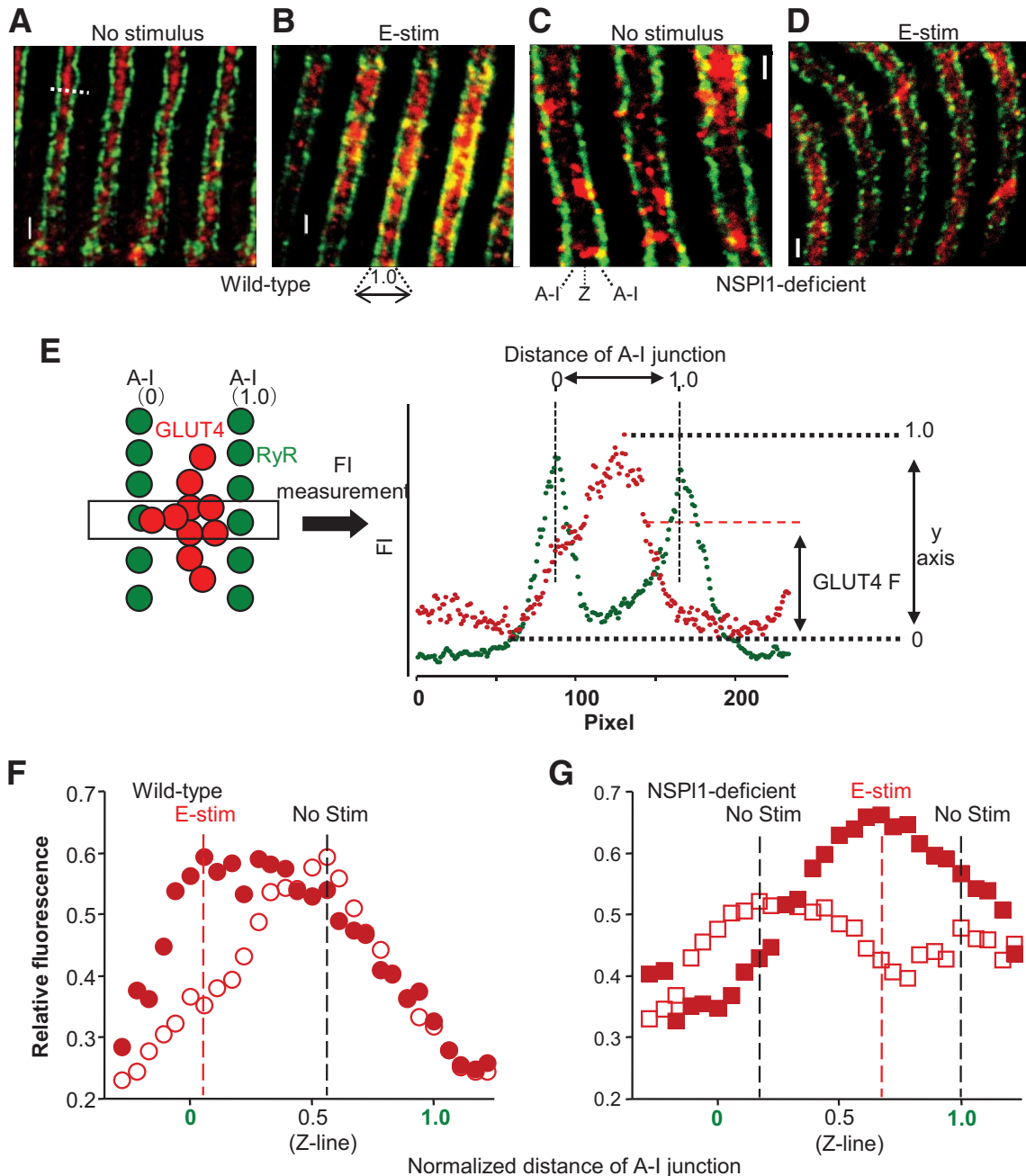


FIG. 5. Distributions of GLUT4 in the transverse tubules. **A–D:** Comparison of the distribution of GLUT4 near the transverse tubules recognized by anti-GLUT4 (red) and anti-ryanodine receptor (green) in the wild-type (**A** and **B**) or sk-NSP11-deficient (**C** and **D**) muscles, without (**A** and **C**) or with (**B** and **D**) electrical stimulation for 15 min. Ryanodine receptor was located very close to the transverse tubules, and thus it was used as the transverse-tubule membrane or A-I junction marker. GLUT4 is located on the transverse tubules or A-I junctions, as seen by the intensity of yellow (**B** and **C**). **E:** Typical quantification of GLUT4 translocation in the transverse tubules. After obtaining the surrounding image, the confocal image at the ryanodine receptor-abundant section was again scanned (12 $\mu\text{m} \times 12 \mu\text{m}$, 2048 \times 2048 pixels) (**A–D**). From the recorded image, distances between two A-I junctions were measured (i.e., the white dashed line shown in **A** and the box illustrated in **E**, 200–350 pixels/line), judging from ryanodine receptor immunofluorescence (green circles), and then normalized (0 and 1.0, horizontal axis in **F** and **G**). Intensities of GLUT4 immunofluorescence along this line (red circles) were also measured, and the means at every 0.06 normalized distance along the line were plotted against the normalized distance of the A-I junction. **F** and **G:** Results of the GLUT4 translocation in the transverse tubules. Black and red dashed lines represent the normalized distance, where the intensity from GLUT4 reached a peak value without or with stimulation, respectively. Wild type: without stimulation, $n = 60$ (couples of transverse tubules from two mice); with stimulation, $n = 71$ (three mice). sk-NSP11 deficient: without stimulation, $n = 67$ (two mice); with stimulation, $n = 55$ (two mice). Bar = 1 μm . E-stim, electrical stimulation; RyR, ryanodine receptor. (A high-quality color digital representation of this figure is available in the online issue.)

heterozygous mice (Fig. 8 and supplemental Fig. 4). In wild-type muscles, sk-NSP11 existed mainly in the region between the A-I junction, as transverse elements over the actin (Fig. 8A–C). Longitudinal elements also existed at constant intervals at low levels. Therefore, the array of NSP11 appears like a lattice (Fig. 8A and supplemental Fig. 4). This characteristic structure was totally abolished in

the sk-NSP11-deficient muscles (Fig. 8G–I), although there is a possibility that non-skeletal type NSP11 remained or increased (supplemental Fig. 4). In heterozygotes, the lattice-like distribution was also recognized; however, only the transverse elements on actin were greatly decreased (Fig. 8D–F), whereas the longitudinal elements remained. Thus, NSP11-heterozygous mice, with abolished exercise-

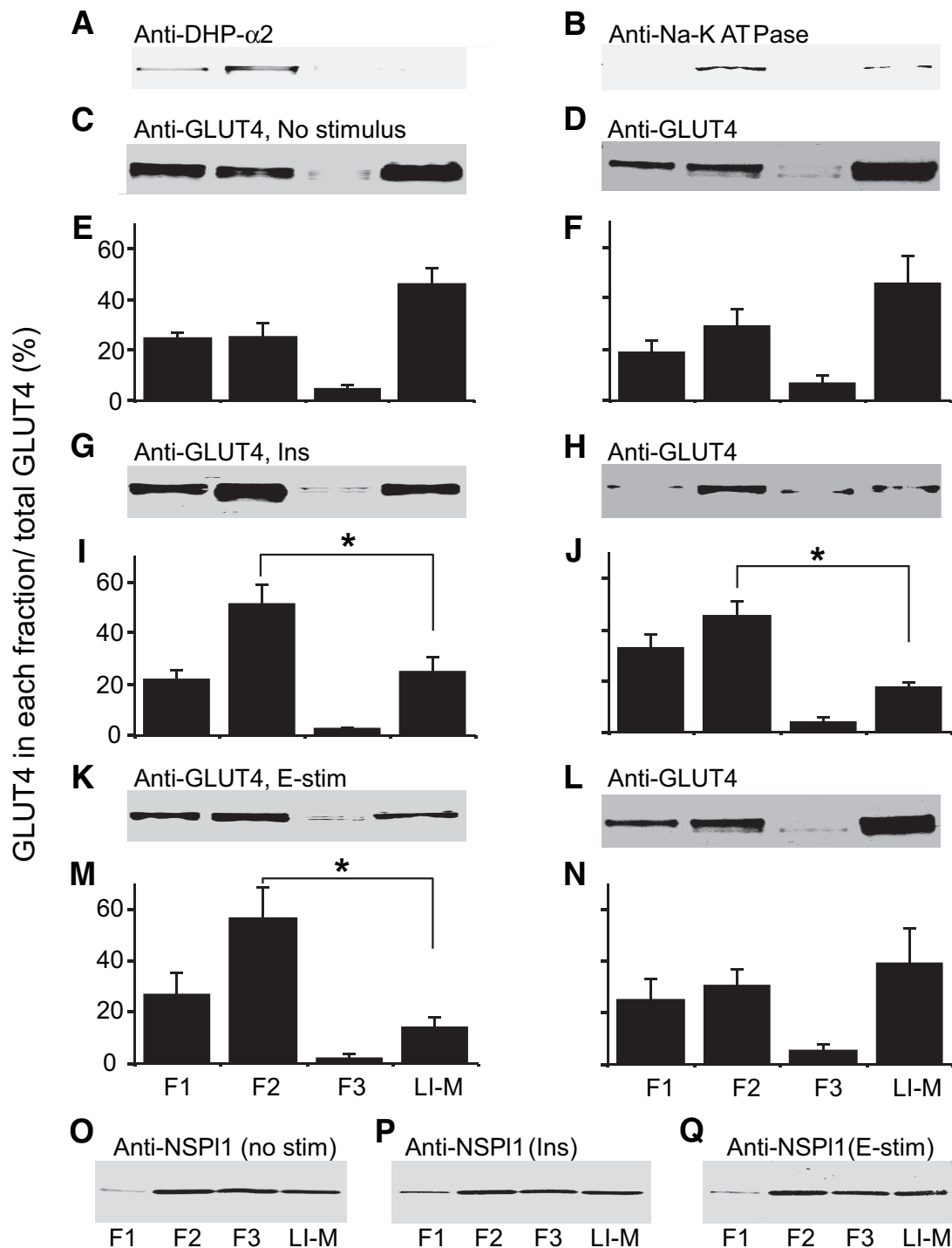


FIG. 6. Membrane translocation of GLUT4 in the isolated membrane from skeletal muscle. **A** and **B**: Distributions of dihydropyridine (DHP) receptor and Na-K ATPase (Na pump) in fractions 1–3 (F1–F3) and LiBr-treated membrane (LI-M) from skeletal muscles. **C–N**: GLUT4 translocation in isolated membrane fractions after anesthesia for 30–45 min without any stimulation (**C–F**), or with insulin (Ins; 2 units) (**G–J**) for 30 min and with electrical stimulation for 15 min (**K–N**) in wild-type (**C** and **E**, **G** and **I**, **K** and **M**, left panels) and sk-NSP11-deficient (**D** and **F**, **H** and **J**, **L** and **N**, right panels) skeletal muscles. Typical results after visualization of GLUT4 protein on PVDF membrane are shown in **C**, **D**, **G**, **H**, **K**, and **L**. The relative content of GLUT4 in each fraction calculated by densitometric counting of total GLUT4 in fraction 1 to LiBr-treated membrane as 100% was compared in **E**, **F**, **I**, **J**, **M**, and **N** ($n = 6$ in each panel). **O–Q**: Constant distribution of sk-NSP11 protein in the membrane fraction with insulin (Ins; 2 units) (**P**), with electrical stimulation (E-stim) (**Q**), or without stimulation (no stim) (**O**). * $P < 0.05$.

induced glucose uptake, showed localized reduction of sk-NSP11 in muscles.

DISCUSSION

In this report, we demonstrated the physiological importance of sk-NSP11 on exercise-induced glucose uptake in skeletal

muscle. Our initial aim was to elucidate the molecular mechanism of excitation-contraction coupling in skeletal muscle. We had hoped to discover a protein that mediates the signal from voltage sensors (dihydropyridine receptor) situated on the transverse-tubule membrane to the ryanodine receptor in the SR membrane using our newly synthesized

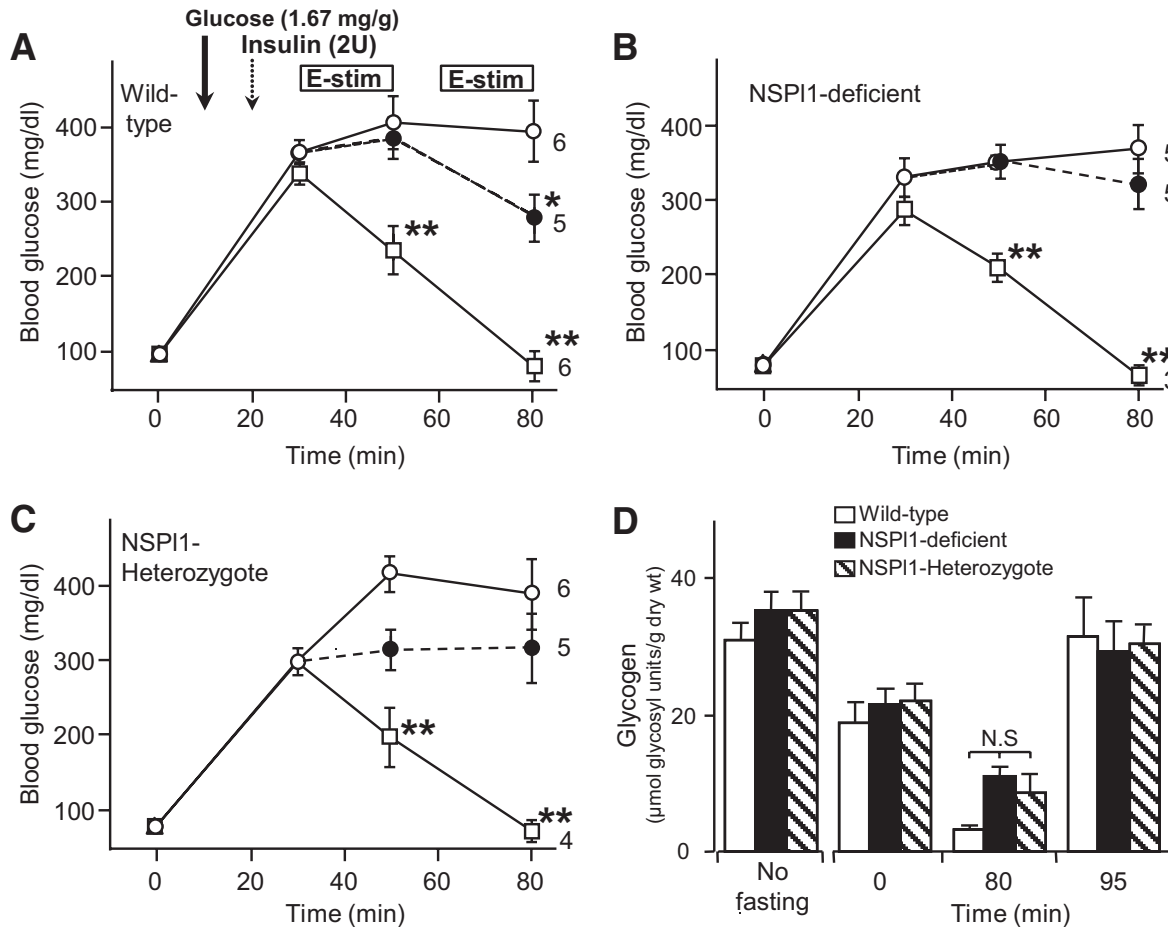


FIG. 7. Effects of different stimulants on blood glucose concentration of mice. *A–C*: Changes in blood glucose concentration were measured in wild-type (*A*), sk-NSP11-deficient (*B*), and NSP11-heterozygous (*C*) mice under anesthesia (8–12 weeks old). After measuring the fasting level of blood glucose concentrations at time = 0, a high concentration of glucose was injected subcutaneously (time = 10 min; bold arrow). Electrical stimulation on the hind limbs was given for 20 min after measuring blood glucose at time = 30 min and again for 20 min after a 10-min interval (E-stim; boxes in *A*). Control (○, high glucose injection alone), electrical stimulation (●) and insulin (□). Numbers of experiments are indicated near each symbol at 80 min. * $P < 0.05$, ** $P < 0.01$ (against control values). *D*: Glycogen level for in situ contractions. Glycogen levels during experiments in *A–C* for femoris muscles (~1.0 cm distance from electrodes, $n = 8–12$) were measured at the time in the abscissa. Glycogen levels without stimulation at 80 min were significantly higher than those with stimulation (80 min, 21.16 ± 1.16 for wild type, $n = 4$, $P < 0.01$; 17.69 ± 0.97 for sk-NSP11 deficient, $n = 4$, $P < 0.05$; 23.57 ± 2.12 for sk-NSP11 heterozygous, $n = 7$, $P < 0.01$). N.S., not significant; 2U, 2 units.

photoaffinity probes (GIF-0082 and GIF-0430). Unexpectedly, the 23-kDa dantrolene-binding protein we discovered (Fig. 1) had no apparent role in the Ca^{2+} release mechanism because the deletion of its gene (sk-NSP11) had no effect on excitation-contraction coupling (Fig. 2 and supplemental Fig. 2). Instead, when electrically stimulated, uptake of [^{18}F]FDG was dramatically reduced in sk-NSP11-deficient muscles (Fig. 3E). Confocal imaging and biochemical data also demonstrated that electrical stimulation of the muscle resulted in no translocation of GLUT4 from intracellular membranes to the cell membrane in our mutant mice (Figs. 4–6). Moreover, sk-NSP11 was expressed mainly in skeletal muscle (Fig. 1E). Taken together, sk-NSP11 appears to play a role in glucose uptake and membrane translocation of GLUT4 during exercise.

It has been reported that a low amount of Ca^{2+} released from the SR, which is not enough to contract the muscle cells, induces the membrane translocation of GLUT4 (9,13,38). Thus, it has been postulated that the slight but definite elevation in Ca^{2+} concentration in the sarcoplasm might initiate GLUT4 translocation, and therefore the inhibitory action of dantrolene on Ca^{2+} release causes the inhibition of exercise-induced glucose uptake (10). However, the

tension evoked by membrane depolarization is not fully abolished even by a high concentration of dantrolene (16,39,40). That is, at least a small amount of Ca^{2+} can be released from SR even in the presence of dantrolene. Thus, it seemed that the effect of dantrolene on Ca^{2+} release is quantitatively in disagreement with its effect on exercise-induced glucose uptake, suggesting that some other factor(s) or mechanism(s) is responsible for dantrolene-induced inhibition of exercise-induced glucose uptake.

Skeletal muscles from our sk-NSP11-deficient mice lost exercise-induced glucose uptake accompanied by membrane translocation of GLUT4 without any severe defect in Ca^{2+} release from the SR. In addition, GIF-0166 and GIF-0192 (22), which have the opposite action of dantrolene, are weak potentiators of Ca^{2+} release (supplemental Fig. 1J and K), but they have affinity to sk-NSP11 (Fig. 1A), which also inhibited [^{18}F]FDG uptake (Fig. 3E). Thus, it is clear that inhibition of exercise-induced glucose uptake by dantrolene is unrelated to the reduction in Ca^{2+} release.

Ca^{2+} may well be involved in a certain step in signal transduction of exercise-induced glucose uptake, for example, in the regulation of AS160 (2,41,42) protein after the activation of Ca^{2+} -calmodulin-dependent protein ki-

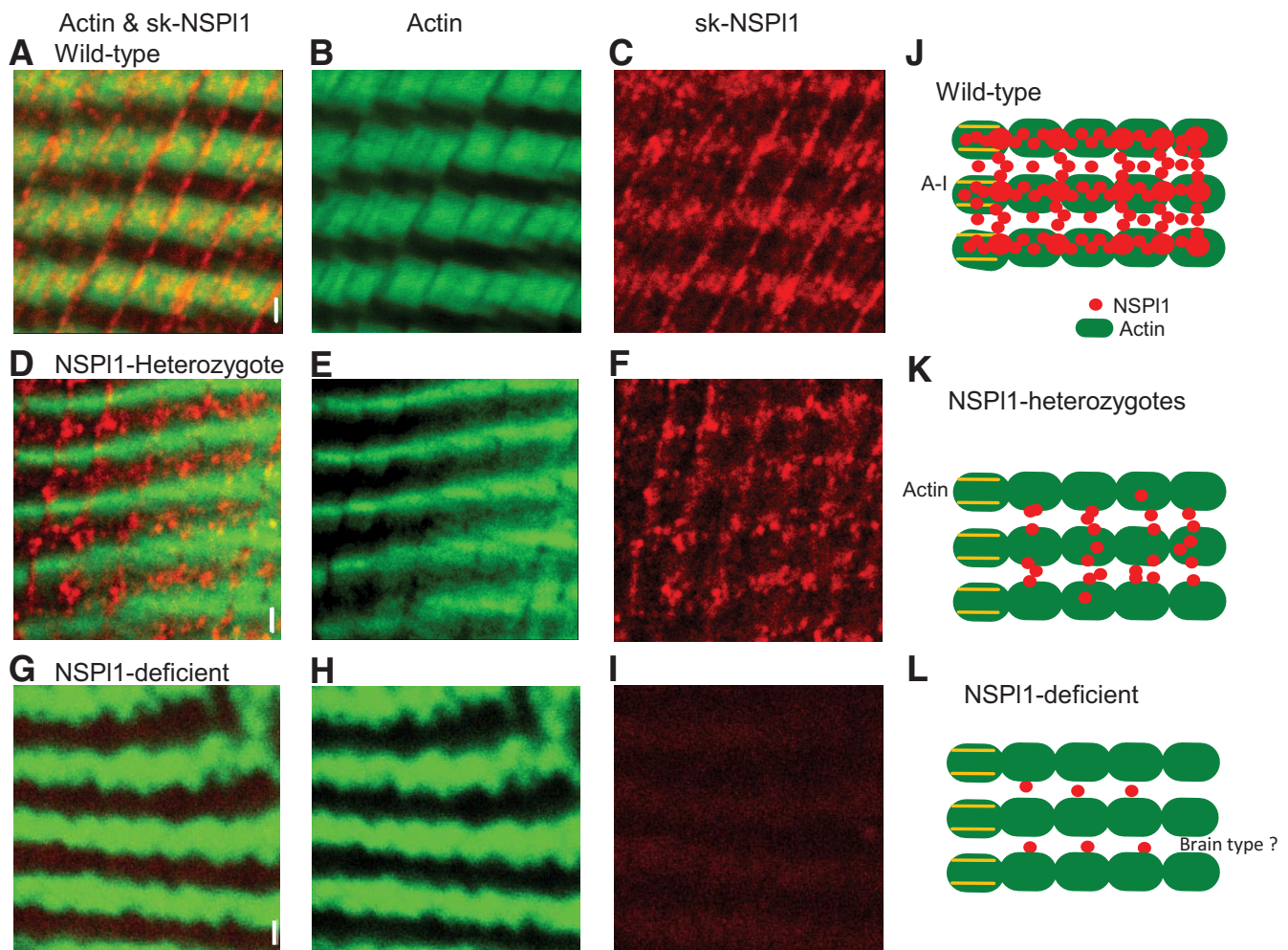


FIG. 8. Localization of sk-NSP11 in skeletal muscles. Actin was labeled with phalloidin conjugated to Alexa Fluor 488 (green). Sk-NSP11 was recognized by its specific antibody and labeled with Alexa Fluor 568-conjugated secondary antibody (red). Confocal images were obtained from muscles (EDL) at sk-NSP11-abundant sections without stimulation ($10 \mu\text{m} \times 10 \mu\text{m}$, $1,024 \times 1,024$ pixels) in wild-type (A–C), sk-NSP11-heterozygous (D–F), and sk-NSP11-deficient muscles (G–I). Bar = $1 \mu\text{m}$. Images are shown of double staining (A, D, and G), actin (B, E, and H), and sk-NSP11 (C, F, and I). Sk-NSP11 was concentrated on the actin in wild-type muscle, as seen by the intensity of yellow (A). J–L: Diagram of localized sk-NSP11 from three genotypes, showing NSP11 (red circle), actin (green filled oval), and A-I junction (transverse tubules; yellow line). (A high-quality color digital representation of this figure is available in the online issue.)

nase (43) or AMP-activated kinase (44–46). However, our results indicated that the main target of dantrolene in exercise-induced glucose uptake is not the ryanodine receptor- Ca^{2+} release channel, but NSP11. NSP11 might be present further downstream of Ca^{2+} -dependent signal transduction in exercise/contraction-dependent glucose uptake. On the other hand, the normal action of insulin preserved in sk-NSP11-deficient skeletal muscles means that insulin-induced glucose uptake is regulated independently of sk-NSP11. In addition, glycogen metabolism in skeletal muscle is also unrelated primarily to the abnormality of our mutants (Figs. 3C and 7D).

Geisler et al. (47) reported that NSP11 is the Z-line protein, using a chimeric green fluorescent protein-NSP11 protein expressed in chick primary myotubes. Recently, an analysis of confocal imaging using endoplasmic reticulum and SR protein markers demonstrated that Z-line-flanking structures are composed within the exporting endoplasmic reticulum (48). Therefore, the sk-NSP11 located in this region (Fig. 8A–C) might take part in the export of vesicles containing GLUT4 protein from the internal membrane. In addition, sk-NSP11 expressed in this region might be the most important factor for GLUT4

translocation because exercise-induced glucose uptake was totally abolished in the homozygotes, and the heterozygotes (Figs. 3E and 7C) lost sk-NSP11 in the transverse elements over actin (Fig. 8). At present, however, we are not able to exclude the involvement of the longitudinal strands discovered in this study (Fig. 8A–C, supplemental Fig. 4A and B). Both of them might be necessary for normal GLUT4 translocation. Longitudinal sk-NSP11 near the sarcolemma might also be involved in endocytosis of GLUT4, in the translocation mechanism in the cell, as reported previously (12).

All of the data in the current report demonstrated the physiological importance of this protein (and gene) in the regulatory system of glucose metabolism. Further information is necessary for understanding the molecular mechanism of sk-NSP11-dependent GLUT4 translocation. Considering that this protein was discovered as a drug (dantrolene) receptor and that it can change blood glucose levels in the whole body (Fig. 7), further study might lead to the development of preventive or therapeutic agents for various types of lifestyle-related diseases, including type 2 diabetes.

ACKNOWLEDGMENTS

This work was supported by the molecular imaging program of Research Base for Exploring New Drugs, from the Ministry of Education, Culture, Sports, Science, and Technology (MEXT), Japan.

No potential conflicts of interest relevant to this article were reported.

REFERENCES

- Huang S, Czech MP. The GLUT4 glucose transporter. *Cell Metabolism* 2007;5:237–252
- Röckl KS, Witczak CA, Goodyear LJ. Signaling mechanisms in skeletal muscle: acute responses and chronic adaptations to exercise. *IUBMB Life* 2008;60:145–153
- Ellis KO, Carpenter JF. Studies on the mechanism of action of dantrolene sodium: a skeletal muscle relaxant. *Naunyn Schmiedeberg's Arch Pharmacol* 1972;275:83–94
- Van Winkle WB. Calcium release from skeletal muscle sarcoplasmic reticulum: site of action of dantrolene sodium. *Science* 1976;193:1130–1131
- Harrison GG. Control of the malignant hyperpyrexia syndrome in MHS swine by dantrolene sodium. *Br J Anaesth* 1975;47:62–65
- Kolb ME, Horne ML, Martz R. Dantrolene in human malignant hyperthermia. *Anesthesiology* 1982;56:254–262
- MacLennan DH, Phillips MS. Malignant hyperthermia. *Science* 1992;256:789–794
- Valant P, Erlj D. K⁺-stimulated sugar uptake in skeletal muscle: role of cytoplasmic Ca²⁺. *Am J Physiol* 1983;245:C125–C132
- Youn JH, Gulve EA, Henriksen EJ, et al. Interactions between effects of W-7, insulin, and hypoxia on glucose transport in skeletal muscle. *Am J Physiol Regul Integr Comp Physiol* 1994;267:R888–R894
- Yu B, Poirier LA, Nagy LE. Mobilization of GLUT-4 from intracellular vesicles by insulin and K⁺ depolarization in cultured H9c2 myotubes. *Am J Physiol* 1999;277:E259–E267
- Ojuka EO, Jones TE, Nolte LA, et al. Regulation of GLUT4 biogenesis in muscle: evidence for involvement of AMPK and Ca²⁺. *Am J Physiol Endocrinol Metab* 2002;282:E1008–E1013
- Wijesekara N, Tung A, Thong F, et al. Muscle cell depolarization induces a gain in surface GLUT4 via reduced endocytosis independently of AMPK. *Am J Physiol Endocrinol Metab* 2006;290:E1276–E1286
- Terada S, Muraoka I, Tabata I. Changes in [Ca²⁺]_i induced by several glucose transport-enhancing stimuli in rat epitrochlearis muscle. *J Appl Physiol* 2003;94:1813–1820
- Park S, Scheffler TL, Gunawan AM, et al. Chronic elevated calcium blocks AMPK-induced GLUT4 expression in skeletal muscle. *Am J Physiol Cell Physiol* 2009;296:C106–C115
- Palnitkar SS, Bin B, Jimenez LS, et al. [³H]azidodantrolene: synthesis and use in identification of a putative skeletal muscle dantrolene binding site in sarcoplasmic reticulum. *J Med Chem* 1999;42:1872–1880
- Ikemoto T, Hosoya T, Aoyama H, et al. Effects of dantrolene and its derivatives on Ca²⁺ release from sarcoplasmic reticulum of mouse skeletal muscle fibres. *Br J Pharmacol* 2001;134:729–736
- Paul-Plutzer K, Yamamoto T, Ikemoto N, et al. Probing a putative dantrolene-binding site on the cardiac ryanodine receptor. *Biochem J* 2005;387:905–909
- Geisler JG, Stubbs LJ, Wasserman WW, et al. Molecular cloning of a novel mouse gene with predominant muscle and neural expression. *Mamm Genome* 1998;9:274–282
- Mitchell RD, Palade P, Fleischer S. Purification of morphologically intact triad structures from skeletal muscle. *J Cell Biol* 1983;96:1008–1016
- Hosoya T, Hiramatsu T, Ikemoto T, et al. Design of dantrolene-derived probes for radioisotope-free photoaffinity labeling of proteins involved in the physiological Ca²⁺ release from sarcoplasmic reticulum of skeletal muscle. *Bioorg Med Chem Lett* 2005;15:1289–1294
- Hosoya T, Aoyama H, Ikemoto T, et al. [¹²⁵I]-N-[(3-azido-5-iodo)benzyl]-dantrolene and [¹²⁵I]-N-[[3-iodo-5-(3-trifluoromethyl-3H-diazirin-3-yl)]-benzyl]dantrolene: photoaffinity probes specific for the physiological Ca²⁺ release from sarcoplasmic reticulum of skeletal muscle. *Bioorg Med Chem Lett* 2002;12:3263–3265
- Hosoya T, Aoyama H, Ikemoto T, et al. Dantrolene analogues revisited: general synthesis and specific functions capable of discriminating two kinds of Ca²⁺ release from sarcoplasmic reticulum of mouse skeletal muscle. *Bioorg Med Chem* 2003;11:663–673
- Hosoya T, Hiramatsu T, Ikemoto T, et al. Novel bifunctional probe for radioisotope-free photoaffinity labeling: compact structure comprised of photospecific ligand ligation and detectable tag anchoring units. *Org Biomol Chem* 2004;2:637–641
- Kameya S, Miyagoe Y, Nonaka I, et al. α 1-Syntrophin gene disruption results in the absence of neuronal-type nitric-oxide synthase at the sarcolemma but does not induce muscle degeneration. *J Biol Chem* 1999;274:2193–2200
- Hosaka Y, Yokota T, Miyagoe-Suzuki Y, et al. α 1-Syntrophin-deficient skeletal muscle exhibits hypertrophy and aberrant formation of neuromuscular junctions during regeneration. *J Cell Biol* 2002;158:1097–1107
- Ikemoto T, Iino M, Endo M. Enhancing effect of calmodulin on Ca²⁺-induced Ca²⁺ release in the sarcoplasmic reticulum of rabbit skeletal muscle fibres. *J Physiol* 1995;487:573–582
- Ikemoto T, Endo M. Properties of Ca²⁺ release induced by clofibrate acid from the sarcoplasmic reticulum of mouse skeletal muscle fibres. *Br J Pharmacol* 2001;134:719–728
- Dombrowski L, Roy D, Marcotte B, et al. A new procedure for the isolation of plasma membranes, T tubules, and internal membranes from skeletal muscle. *Am J Physiol* 1996;270:E667–E676
- Ito Y, Obara SK, Ikeda R, et al. Passive stretching produces Akt- and MAPK-dependent augmentations of GLUT4 translocation and glucose uptake in skeletal muscles of mice. *Pflügers Arch* 2006;451:803–813
- Roebroek AJ, Contreras B, Pauli IG, et al. cDNA cloning, genomic organization, and expression of the human RTN2 gene, a member of a gene family encoding reticulons. *Genomics* 1998;51:98–106
- Endo M, Ikemoto T. Regulation of ryanodine receptor calcium release channels. In *Pharmacology of Ionic Channel Function: Activators and Inhibitors. Handbook of Experimental Pharmacology*. Vol. 147. Endo M, Kurachi Y, Mishina M, Eds. Heidelberg, Germany, Springer-Verlag, 2000, p. 581–601
- Williams MW, Bloch RJ. Differential distribution of dystrophin and beta-spectrin at the sarcolemma of fast twitch skeletal muscle fibers. *J Muscle Res Cell Motil* 1999;20:383–393
- Rybakova IN, Patel JR, Ervasti J. The dystrophin complex forms a mechanically strong link between the sarcolemma and costameric actin. *J Cell Biol* 2000;150:1209–1214
- Marette A, Burdett E, Douen A, et al. Insulin induces the translocation of GLUT4 from a unique intracellular organelle to transverse tubules in rat skeletal muscle. *Diabetes* 1992;41:1562–1569
- Ploug T, van Deurs B, Ai H, et al. Analysis of GLUT4 distribution in whole skeletal muscle fibers: identification of distinct storage compartments that are recruited by insulin and muscle contractions. *J Cell Biol* 1998;142:1429–1446
- Lauritzen HP, Ploug T, Prats C, et al. Imaging of insulin signaling in skeletal muscle of living mice shows major role of T-tubules. *Diabetes* 2006;55:1300–1306
- Paolini C, Protasi F, Franzini-Armstrong C. The relative position of RyR feet and DHPR tetrads in skeletal muscle. *J Mol Biol* 2004;342:145–153
- Youn JH, Gulve EA, Holloszy JO. Calcium stimulates glucose transport in skeletal muscle by a pathway independent of contraction. *Am J Physiol Cell Physiol* 1991;260:C555–C561
- Hainaut K, Desmedt JE. Effect of dantrolene sodium on calcium movements in single muscle fibres. *Nature* 1974;252:728–730
- Szentesi P, Collet C, Sárközi S, et al. Effects of dantrolene on steps of excitation-contraction coupling in mammalian skeletal muscle fibers. *J Gen Physiol* 2001;118:355–375
- Sano H, Kane S, Sano E, et al. Insulin-stimulated phosphorylation of a Rab GTPase-activating protein regulates GLUT4 translocation. *J Biol Chem* 2003;278:14599–14602
- Bruss MD, Arias EB, Lienhard GE, et al. Increased phosphorylation of Akt substrate of 160 kDa (AS160) in rat skeletal muscle in response to insulin or contractile activity. *Diabetes* 2005;54:41–50
- Witczak CA, Fujii N, Hirshman MF, et al. Ca²⁺/calmodulin-dependent protein kinase kinase- α regulates skeletal muscle glucose uptake independent of AMP-activated protein kinase and Akt activation. *Diabetes* 2007;56:1403–1409
- Merrill GF, Kurth EJ, Hardie DG, et al. AICA riboside increases AMP-activated protein kinase, fatty acid oxidation, and glucose uptake in rat muscle. *Am J Physiol* 1997;273:E1107–E1112
- Wright DC, Hucker KA, Holloszy JO, et al. Ca²⁺ an AMPK both mediate stimulation of glucose transport by muscle contractions. *Diabetes* 2004;53:330–335
- Sakamoto K, McCarthy A, Smith D, et al. Deficiency of LKB1 in skeletal muscle prevents AMPK activation and glucose uptake during contraction. *EMBO J* 2005;24:1810–1820
- Geisler JG, Palmer RJ, Stubbs LJ, et al. Nsp1, a new Z-band-associated protein. *J Muscle Res Cell Motil* 1999;20:661–668
- Kaisto T, Metsikkö K. Distribution of the endoplasmic reticulum and its relationship with the sarcoplasmic reticulum in skeletal myofibers. *Exp Cell Res* 2003;289:47–57